Colloid Polym Sci (2010) 288:981–989
DOI 10.1007/s00396-010-2218-6

ORIGINAL CONTRIBUTION

Dissipative crystallization of poly-D-lysine hydrobromide, poly-L-lysine hydrobromide, and their low-molecular-weight analogs

Tsuneo Okubo · Junichi Okamoto · Akira Tsuchida

Received: 31 January 2010 / Accepted: 30 March 2010 / Published online: 27 April 2010

Abstract Drying dissipative structures of aqueous solutions of poly-D-lysine hydrobromide, poly-L-lysine hydrobromide, and their low-molecular-weight analogs were studied on a cover glass, a watch glass, and a Petri glass dish. Size of the broad rings, one of the typical macroscopic patterns, decreased as the solute concentration decreased. Microscopic drying crystal patterns of polylysine hydrobromides and their low-molecular-weight analogs, i.e., D-, L-, and DL-lysine hydrochloride changed as a function of the distance from the film center, which is one of the typical features of *dissipative crystallization*. Macroscopic and microscopic drying patterns were quite similar to each other irrespective of their stereospecificity. The crystal patterns of the mixtures of poly-D-lysine hydrobromide and poly-L-lysine hydrobromide were also similar to those of the corresponding single-component polymers. The stereospecific effects were not observed in this work.

Keywords Poly-D-lysine hydrobromide · Poly-L-lysine hydrobromide · Dissipative crystallization · Dissipative structure · Drying pattern · Optical isomer

Electronic supplementary material The online version of this article (doi:10.1007/s00396-010-2218-6) contains supplementary material, which is available to authorized users.

T. Okubo (✉)
Institute for Colloidal Organization,
Hatoyama 3-1-112,
Uji, Kyoto 611-0012, Japan
e-mail: okubotsu@ybb.ne.jp

T. Okubo
Graduate School of Science and Technology,
Yamagata University,
Johnan 4-3-16,
Yonezawa, Yamagata 992-8510, Japan

J. Okamoto · A. Tsuchida
Department of Applied Chemistry, Gifu University,
Yanagido 1,
Gifu 501-1193, Japan

Introduction

Most structural patterns in nature form via self-organization accompanied with the *dissipation* of free energy and in the non-equilibrium state. In order to understand the mechanisms of the dissipative self-organization of the simple model systems, instead of the much complex nature itself, the authors have studied the *convectional*, *sedimentary*, and *drying* dissipative patterns during dryness of colloidal suspensions and solutions as systematically as possible, though these three kinds of patterns are correlated strongly and overlapped each other [1–3].

Typical *convectional* patterns are *Benard cell* [4, 5], the *hexagonal circulating* pattern, and *Terada cell* [6–8], the spoke lines spreading the whole liquid surface accompanied with the huge number of cell convections in the normal direction of the spoke lines. These convectional patterns were observed often in the intermediate and final steps in the convectional processes [9–17]. Recently, the whole processes of the convectional patterns have been clarified experimentally [11, 13, 14]. Theoretical studies of the convectional patterns have been reported mainly using Navier–Stokes equations [18–23]. However, these are not always successful yet when the theories are compared with the experiments.

Sedimentary dissipative patterns during the course of drying suspensions have been studied in detail on a cover glass, a watch glass, a glass dish, and others, for the first time, in our laboratory [11, 24–31]. The broad ring-like patterns were formed in suspension state. It was clarified that the sedimentary particles were suspended above the substrate by the electrical double layers around the particles and always moved by the balancing of the force fields between convectional flow and sedimentation. Quite recently, dynamic bundle-like sedimentary patterns formed cooperatively from the spoke-like convectional structures of coffee [13] and black tea [14] coexisted with cream.

Drying dissipative patterns have been studied for many kinds of colloidal particles [9, 10, 13–17, 24–46], linear-type synthetic and bio-polyelectrolytes [47–49], water-soluble neutral polymers [50, 51], ionic and non-ionic detergents [40, 52, 53], gels [54], colloidal polymer complex [55], and dyes [56]. The macroscopic broad ring patterns of the hill accumulated with the solutes formed. The broad rings moved inward when solute concentration decreased and/or solute size increased. For the non-spherical particles, the round hill was formed in the central area in addition to the broad ring. Macroscopic spoke-like cracks or fine hills including flickering spoke-like ones were also observed for many solutes. Beautiful fractal patterns such as the branch-like, arc-like, block-like, star-like, cross-like, and string-like ones were observed in the microscopic scale.

One of the important findings in our experiments is that the primitive vague sedimentary patterns were formed already in the concentrated suspensions or solutions before dryness and they grew toward fine structures in the process of solidification. It has also been clarified that *information* of the suspensions and solutions, shape and size of solute, and the atmospheric humidity and temperature, for example, is *transferred* into the drying patterns. Furthermore, *dissipative crystallization* of poly(allylamine hydrochloride) [47], poly(ethylene glycol) [57], and sodium salt of poly(methacrylic acid) [58] was newly studied in detail. Accumulation, uneven distribution, symmetric distribution and ordering of the polymer single crystals, and further coupling of the single crystals with the dissipative broad ring patterns have been observed.

The drying dissipative patterns of poly-L-lysine hydrobromide have been studied several years ago by the author's laboratory [48] where the city road-like microscopic patterns were observed. These patterns supported the formation of the crystal structure in the whole process of dryness at the air–liquid and liquid–substrate interfaces. In this work, dissipative crystallization of poly-D-lysine hydrobromide, poly-L-lysine hydrobromide, and their low-molecular-weight analogs is studied in detail. The main purpose of this work was to know the relationship between the dissipative crystallization and the molecular stereospecificity.

Experimental

Materials

D(−)-Lysine monohydrochloride (DLHCl), L(+)-lysine hydrochloride (LLHCl), and DL-lysine monohydrochloride (DLLHCl) were purchased from Wako Pure Chemical Ind. Ltd. (Osaka) and used without further purification. Of the stock solution, 0.1 M was prepared first. Poly-D-lysine hydrobromide (PDLHBr, molecular weight (MW)= 30,000–70,000) and poly-L-lysine hydrobromide (PLLHBr, MW=30,000–70,000) were obtained from Wako and used without further purification. The concentration of the stock solution was 0.01 monoM for the polymers. The water used for the sample preparation was purified by a Milli-Q reagent grade system (Advantage A10, Millipore Co., Bedford, MA, USA).

Observation of the dissipative structures

Aliquot (0.1 ml) of the sample solution was placed carefully and gently onto a micro-cover glass (30× 30 mm, no. 1, thickness 0.12–0.17 mm, Matsunami Glass, Kishiwada, Osaka) set in a plastic dish (type NH-52, 52 mm in diameter, 8 mm in depth, As One Co., Tokyo). The cover glass was used without further rinsing. Four milliliters of the solution was set on a watch glass (70 mm, TOP Co. Tokyo). Five milliliters of the solution was put into a medium glass dish (42 mm in inner diameter and 15 mm in height, code 305-02, TOP Co.). The disposable serological pipettes (1 and 10 ml, Corning Lab. Sci., Co.) were used for putting the suspension in the substrates. The patterns during the course of dryness were observed for the solutions on a desk covered with a black plastic sheet. The room temperature was regulated at 24 °C. Humidity of the room was not regulated and was between 47% and 58%.

Macroscopic patterns were observed on a Canon EOS 10 D digital camera with a macro-lens (EF 50 mm, f=2.5) plus a life-size converter EF or a zoom-lens (Canon, EF28-70 mm, 1:2.8) on a cover glass and a glass dish or a watch glass, respectively. Microscopic drying patterns were observed with a metallurgical microscope (PME-3, Olympus Co., Tokyo). Thickness profiles of the dried films on a cover glass were measured on a laser 3D profile microscope (type VK-8500, Keyence Co., Osaka, Japan). pH measurements of the sample solutions were made on a pH meter (type HM-21P, DKK-TOA Co., Tokyo)

connected with a pH glass electrode (type GST-2729C, DKK-TOA).

Results and discussion

Macroscopic and microscopic dissipative drying patterns of low-molecular-weight analogs of polylysine

Figure 1a, b shows the typical examples of the macroscopic and corresponding microscopic drying patterns of DLHCl (a, d, g), LLHCl (b, e, h), and DLLHCl (c, f, i) on a cover glass (a–c), a watch glass (d–f), and a glass dish (g–i), respectively, at the solute concentration at 0.01 M. pH values of DLHCl, LLHCl, and DLLHCl at 0.001–0.1 M were 6.8, 6.7, and 6.8, respectively. The broad ring patterns were always recognized irrespective of the substrates used (see Fig. 1a for example) and the initial polymer concentrations ranging from 1×10^{-5} to 0.01 monoM. Sizes of the broad rings (d_f) were very small compared with that of the initial liquid (d_i) and decreased as the solute concentration decreased. Figure 2a shows the d_f/d_i values of DLHCl, LLHCl, and DLLHCl as a function of the solute concentration. Here, the size of the broad rings was measured as the distance between the outside edges, not the thickness peak positions of the broad rings. The ratios were quite similar to each other among the various stereospecific solutes, though those seems to increase in the order of cover glass < watch glass < glass dish depending on the substrates used. Increase in the broad ring size with the concentration is due to the fact that the inter-solute crystalline structure is formed within the small areas when the solute concentration is low. Small size of the broad ring of solutes of the low molecular weights or small size of colloidal particles has also been observed so often [15–17, 28, 29, 40, 57, 59]. This is mainly due to the very small excluded volumes of the small solutes compared with the large ones. It should be noted that the concentration and size dependencies of the broad ring do not support the *pinning effect* of the contact line proposed by Deegan et al. [22].

Figure 1b shows the typical examples of the microscopic patterns of DLHCl, LLHCl, and DLLHCl on a cover glass, a watch glass, and a glass dish, respectively. At first glance, the morphologies of the optical isomers look different from each other in Fig. 1b. However, it should be noted here that the morphology of the dissipative crystals, which form in the course of drying processes on the substrate, differ as a function of the distance from the center of the dried film [15–17, 48, 57, 58]. The typical examples of the dissipative microscopic patterns of DLHCl are shown in Electronic supplementary materials (ESM) Fig. 1c. Morphology of the crystal changes clearly as a function of the distance from the center. However, the lattice structure itself should be the same irrespective of the distance. Thus, these morphological differences in Fig. 1b are due to the *dissipative effect* during the drying process and not due to the *stereospecific effect* (Fig. 2).

The similar comparison among the different optical isomers and substrates like Fig. 1b was made at the solute concentrations of 0.001 and 0.1 M, though the graphs showing these are omitted in this paper to save space. When the differences in the dissipative effect on the microscopic patterns are taken into account, any difference in the stereospecific effect was not observed clearly.

Typical examples of the macroscopic and microscopic drying patterns of the mixtures of DLHCl and LLHCl are shown in Fig. 3a, b (ESM), respectively. Total concentration of mixtures is kept at 0.1 M in the pictures. Clearly, both the macroscopic and microscopic patterns were quite similar in the essential aspects of the morphology irrespective of the mixing rations. Any special interaction between DLHCl and LLHCl, complex formation, for example, was not deduced.

Macroscopic and microscopic dissipative drying patterns of poly-D-lysine hydrobromide and poly-L-lysine hydrobromide and their mixtures

Typical examples of the macroscopic and microscopic dissipative crystallization patterns of PDLHBr (a, d, g), PLLHBr (b, e, h), and their 1:1 mixtures (c, f) at 0.01 monoM are shown in ESM Fig. 4a–c on a cover glass (a–c), a watch glass (d–f), and a glass dish (g, h). The pH values of all the sample solutions were 6.6 at any concentrations between 1×10^{-6} and 0.01 monoM. The broad rings were always observed at the outside edge of the dried film for a cover glass and a watch glass and at the inner area from the cell wall for a glass dish, respectively (see *g* and *h* of Fig. 4a). The macroscopic patterns look surprisingly similar to each other irrespective of the stereospecificity of the polymer and also of the substrates. The mixtures of D- and L-isomers also showed quite similar patterns of the single component of polymers. As is clear in ESM Fig. 4b, the microscopic patterns in the outside edge area were quite similar to each other among D- and L-isomers and their mixtures. The microstructure of the mixture on a cover glass in the middle areas between the central and the outside edge looks different from those of single-component polymers, dendritic, and city road-like, respectively. These differences in the patterns are, however, due to the dissipative effect during the drying processes and not due to the stereospecific effect as described above. Morphologies of the polymer crystals in the middle areas look different depending on the substrates, as is shown in ESM Fig. 4c. These differences are again due to the dissipative effect in the different experimental

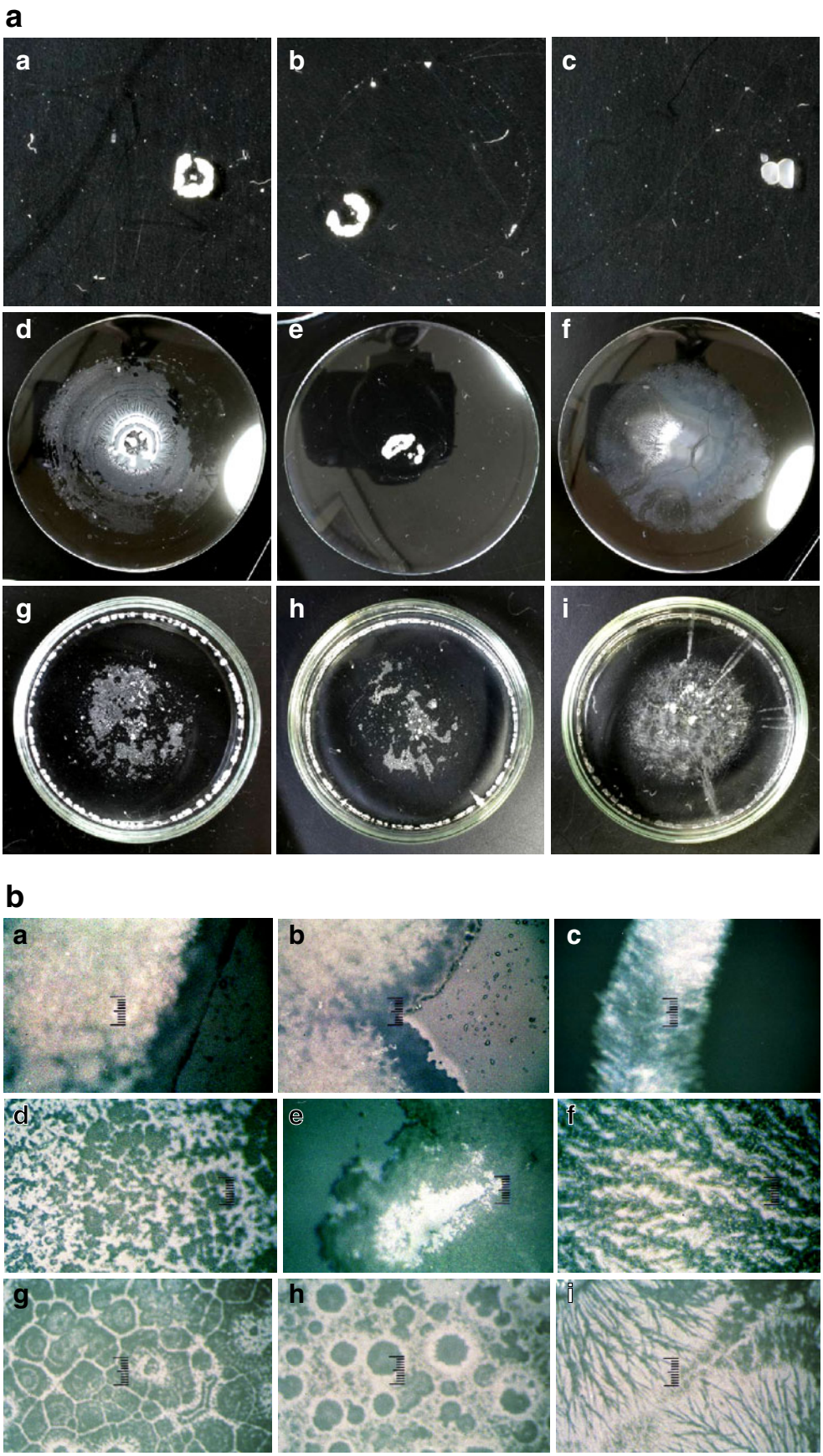

Fig. 1 **a** Drying dissipative patterns of aqueous DLHCl (*a*, *d*, *g*), LLHCl (*b*, *e*, *h*), and *DL*LHCl (*c*, *f*, *i*) on a cover glass (*a–c*), a watch glass (*d–f*), and a Petri glass dish (*g–i*) at 24 °C at 0.01 M. **b** Microscopic drying dissipative patterns of aqueous DLHCl (*a*, *d*, *g*), LLHCl (*b*, *e*, *h*), and *D*LLHCl (*c*, *f*, *i*) on a cover glass (*a–c*), a watch glass (*d–f*), and a Petri glass dish (*g–i*) at 24 °C at 0.01 M

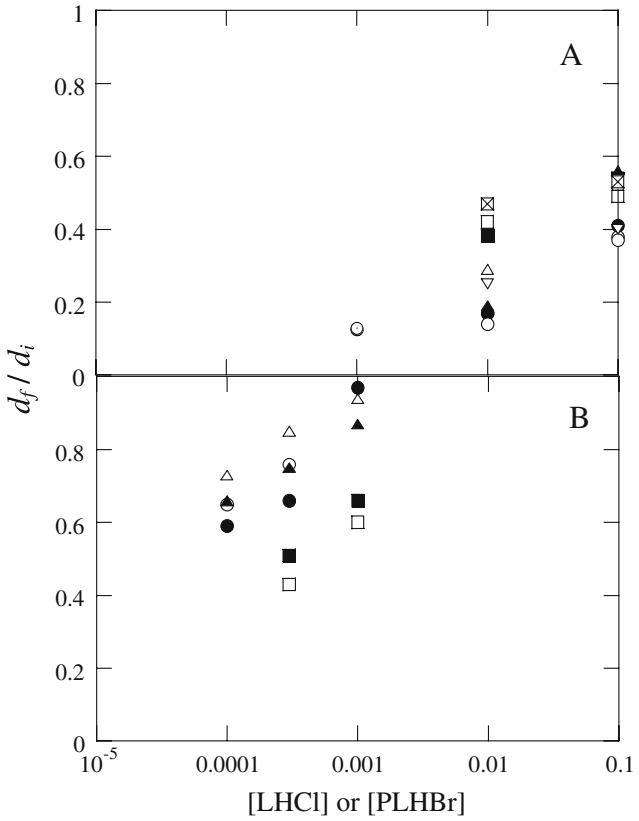

Fig. 2 **a** Plots of d_f/d_i of DLHCl (*open circle*, *open triangle*, *open square*), LLHCl (*closed circle*, *closed triangle*, *closed square*) and DLLHCl (⊙, ▽, ⊠) as a function of polymer concentration on a cover glass (○, ●, ⊙), a watch glass (*open triangle*, *closed triangle*, *inverted triangle*) and a Petri glass dish (□, ■, ⊠) at 24 °C. **b** Plots of d_f/d_i of PDLHBr (*open circle*, *open triangle*, *open square*) and PLLHBr (*closed circle*, *closed triangle*, *closed square*) as a function of polymer concentration on a cover glass (*open circle*, *closed circle*), a watch glass (*open triangle*, *closed triangle*), and a Petri glass dish (*open square*, *closed square*) at 24 °C

conditions of the amount of polymer solution, shape of substrate, and proceeding direction of drying frontier, for example. It should be noted here that the city road-like microscopic patterns were observed already in our previous work [48]. It should be further noted that most of the polymer solutes are accumulated at the broad ring area and quite few molecules locate in the middle area in the dried film.

Size of the broad rings of PDLHBr and PLLHBr increased as polymer concentration increased, as is shown in Fig. 2b, though the experimental errors are rather large. This size effect is clearly shown for PDLHBr and PLLHBr in Fig. 5a, b (in ESM). Figure 2b shows the plots of d_f/d_i of PDLHBr and PLLHBr as a function of polymer concentration. Several important findings are clear. Firstly, the d_f/d_i values are fairly large compared with those of their low-molecular-weight analogs. This has been observed often as described above and is due to the very large excluded volumes of the extended polyelectrolytes compared with those of the low-molecular-weight analogs. Secondly, the ratios increased as polymer concentration increased, which have been observed always without exception. It should be recalled that the broad ring formation of PLLHBr has been observed previously by our group [48]. Below the critical polymer concentration, m^* (around 0.01 monoM in the initial polymer concentration), broad ring size of the drying pattern (d_f) of PLLHBr was small compared with that of the initial solution (d_i) and increased with polymer concentration. Furthermore, the m^* value agreed excellently with the critical polymer concentration where the surface tensions started to decrease sharply as polymer concentration increased. Thirdly, the ratios of the D-isomers look larger than those of L-isomers on a cover glass and a watch glass, whereas the order is reversed on a glass dish. However, these differences are not so reliable because the experimental errors are estimated to be rather large.

Typical example of the change of patterns as a function of the distance from the center of the drying film is shown in Fig. 6 for PDLHBr in a watch glass. The patterns changed from the *city road*-like to *dendritic* and then to the *ring-like arrays of the blocks* from the central region to the outside edge. This change is one of the typical features of the dissipative crystallization. It should be noted here that the change in the patterns with the distance from the film center was observed clearly for the polymers compared with the corresponding low-molecular-weight analogs. It should be further noted here that the ring-like arrays of the blocks at the broad ring area outside edge of the dried film, where most of the polymer molecules are accumulated, are the typical crystal structure formed naturally without strong dissipative effects. On the other hand, the city road-like and dendritic crystal structures form among a small amount of polymer molecules at the middle areas under strong dissipative effects such as strong interaction of the polymer molecules with the interface of the substrate and the convectional shear forces resulting the orientation of the molecules during the drying process. In other words, it is highly plausible that the dissipative crystalline structures appear much more often in the thin middle area of the dried film compared with the very thin broad ring area.

Let us discuss the drying patterns of the mixtures of the stereo-isomers in detail. The macroscopic patterns of the mixtures of PDLHBr and PLLHBr with the mixing ratios of 1:0, 3:1, 1:1, 1:3, and 0:1 are shown in Fig. 7a at the polymer concentrations 0.001 monoM (a–e) and 0.01 monoM (f–j). The broad ring patterns are observed clearly irrespective of the mixing ratios. Their sizes are also insensitive to the ratios when the experimental errors are taken into account. Colors of the broad rings look whiter for the mixtures than those of the single-component polymers. This difference in the colors may support that the solubility of the mixtures in water are slightly low

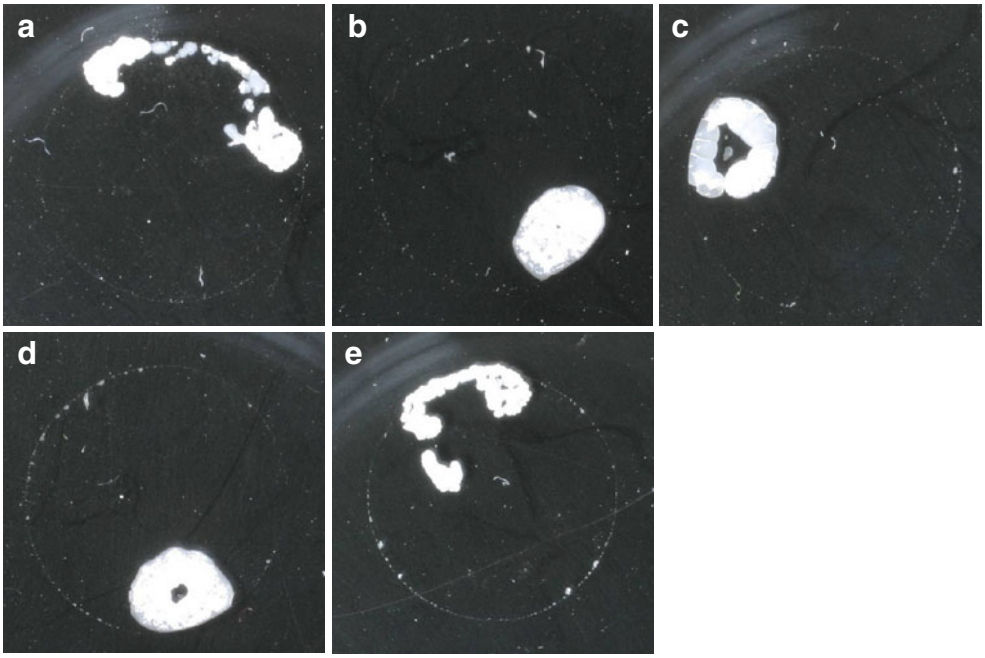

Fig. 3 **a** Drying dissipative patterns of aqueous DLHCl + LLHCl on a cover glass at 24 °C. 0.1 ml, [DLHCl] + [LLHCl] = 0.1 M. [*D*LHCl]/[*L*LHCl] = *a* 1:0, *b* 3:1, *c* 1:1, *d* 1:3, *e* 0:1

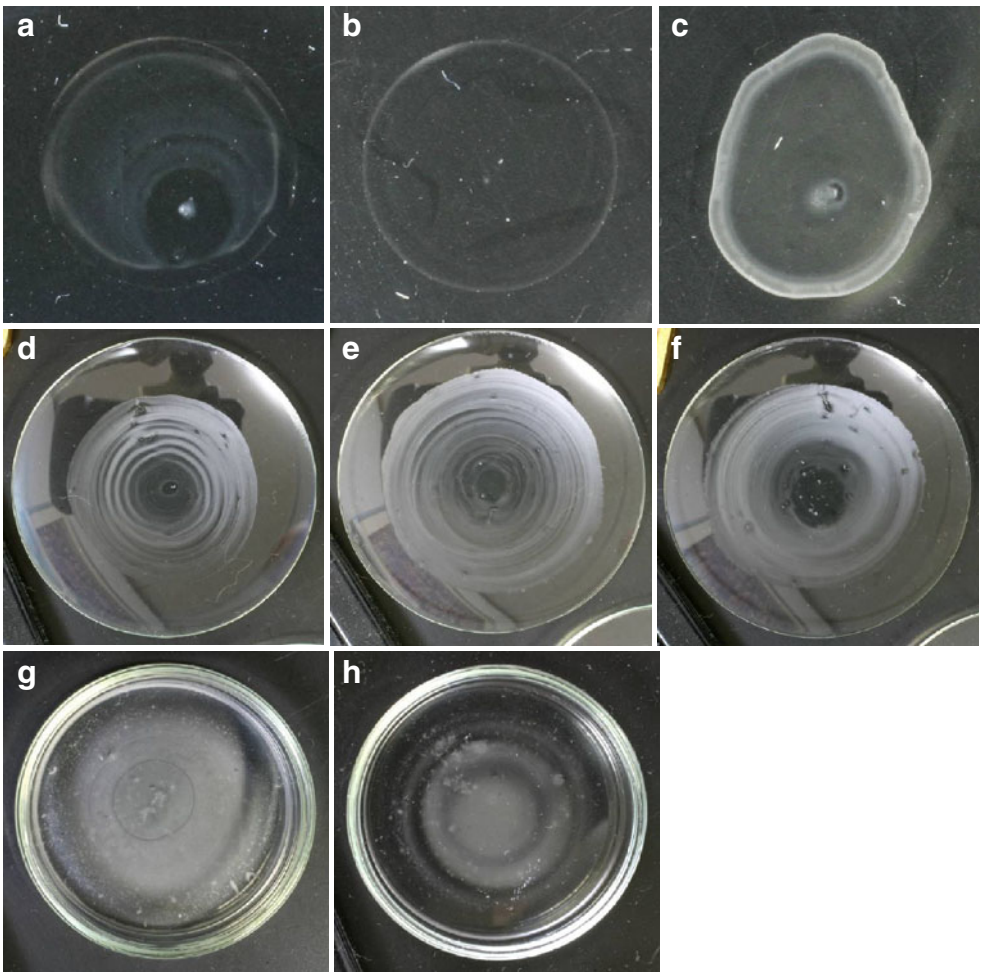

Fig. 4 **a** Drying dissipative patterns of aqueous PDLHBr (*a*, *d*, *g*), PLLHBr (*b*, *e*, *h*), and PDLHBr + PLLHBr (*c*, *f*) on a cover glass (*a–c*), a watch glass (*d–f*), and a Petri glass dish (*g*, *h*) at 24 °C at 0.01 M

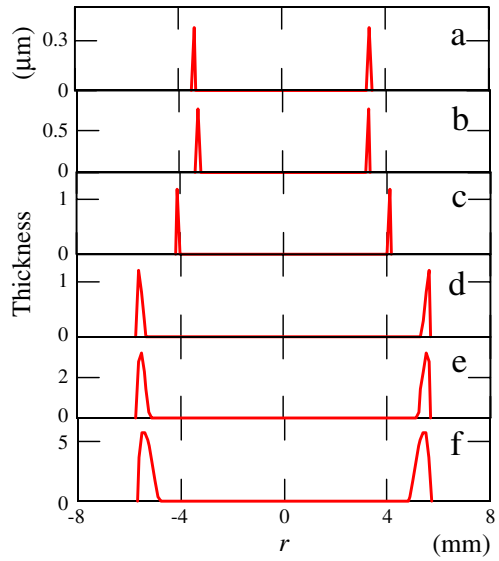

Fig. 5 **a** Thickness profiles of the dried films of PDLHBr as a function of the distance from the center on a cover glass at 24 °C. 0.1 ml [PDLHBr] = *a* 1×10^{-5} monoM, *b* 1×10^{-4} monoM, *c* 3×10^{-4} monoM, *d* 0.001 monoM, *e* 0.003 monoM, *f* 0.01 monoM

compared with those of the single-component polymers, though this speculation has no evidences yet.

The distinct differences in the microscopic patterns between the single-component polymers and the mixtures were observed in ESM Fig. 7b, typical examples of the microscopic patterns at the edge and the middle areas and further at 0.001 and 0.01 monoM of the total polymer concentration. For the patterns in the outside edge areas, the microscopic patterns at 0.01 monoM were ring-like arrays of the blocks irrespective of the mixing ratios. On the other hand, in the microscopic patterns at the middle areas and at 0.001 monoM, the mixtures showed dendritic, whereas most of the patterns of both PDLHBr and PLLHBr were crossed road-like. These changes in the microcrystal structure by mixing is due to the *dissipative* effect as described above and may not support the specific interactions between the stereo-isomers, i.e., stereo-complex formation between PDLHBr and PLLHBr. Stereo-complexation between the anionic polyelectrolytes of D- and L-isomers is considered to be difficult due to the electrostatic repulsion forces between the macroions. As is well known, typical example of the stereo-complexation in polymer system is between poly(D-lactic acid) and poly (L-lactic acid) in chloroform in the undissociated conditions [59, 60]. Any distinct differences between the stereo-isomers were not observed on a watch glass (Fig. 8).

The drying patterns of PLLHBr were further observed on a cover glass at pH 8.3 and 10.5 by adding NaOH into the stock solution. Typical examples of the macroscopic and microscopic drying patterns are shown in ESM Fig. 9a, b, respectively. The macrostructures at 8.3 were quite similar to those of the solutions at pH 6.6 without NaOH addition.

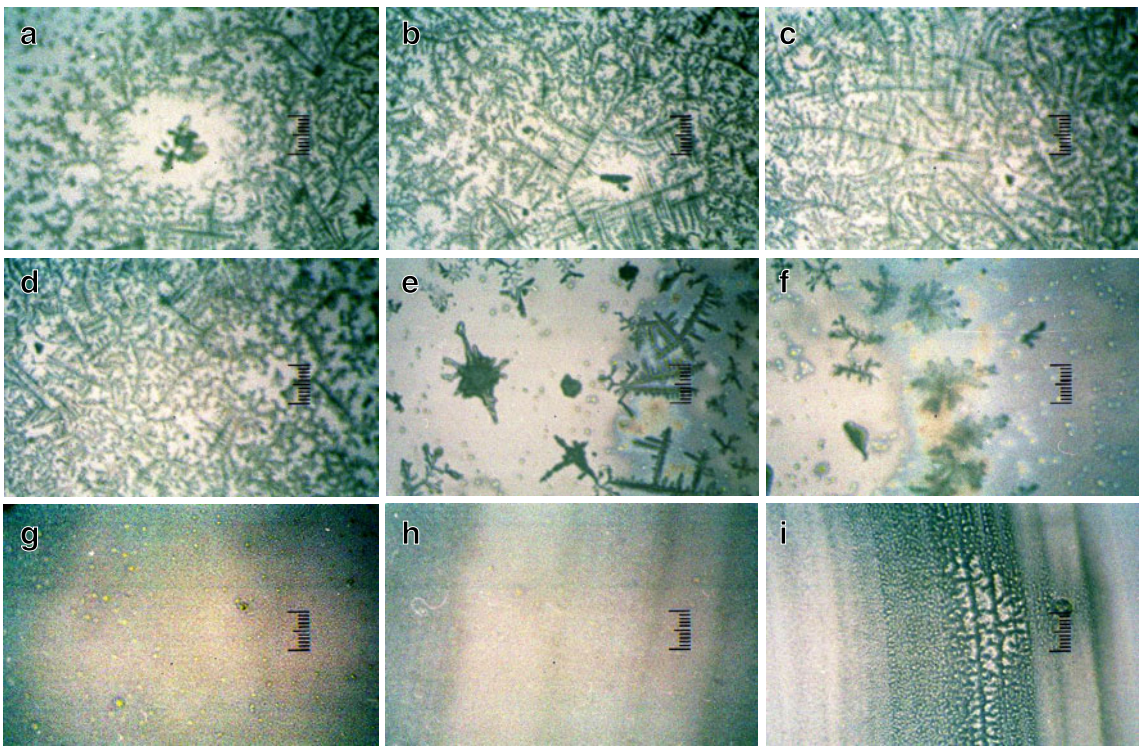

Fig. 6 Microscopic drying dissipative patterns of aqueous PDLHBr on a watch glass at 24 °C. 4 ml [PDLHBr] = 0.0003 monoM. *a–f* Pictures from the center to the right edge; full scale is 100 μm

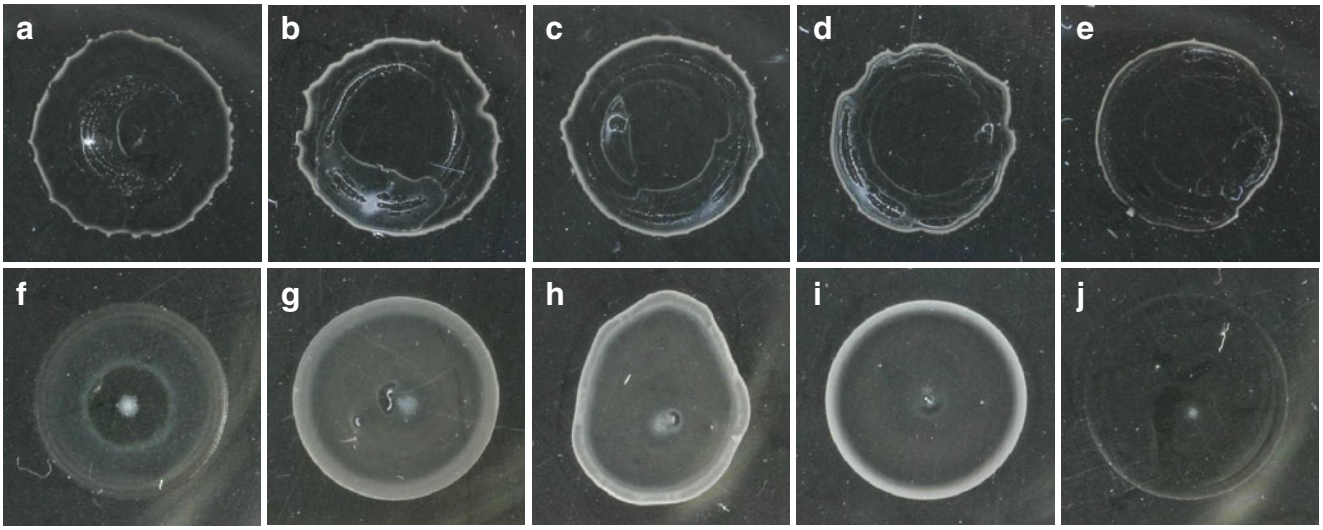

Fig. 7 **a** Drying dissipative patterns of aqueous PDLHBr + PLLHBr on a cover glass at 24 °C. 0.1 ml. *a* [PDLHBr + PLLHBr] = 0.001 monoM, [PDLHBr]/[PLLHBr] = 1:0, *b* 3:1, *c* 1:1, *d* 1:3, *e* 0:1. *f* [PDLHBr + PLLHBr] = 0.01 monoM, [PDLHBr]/[PLLHBr] = 1:0, *g* 3:1, *h* 1:1, *i* 1:3, *j* 0:1

The broad rings of the macroscopic patterns at pH 10.5 were whitey especially at high polymer concentrations, though the patterns themselves were quite insensitive to the pH values (see ESM Fig. 9a). Microstructures at pH 8.3 and 10.5 were also quite similar to those of the solutions at pH 6.6. Macroscopic and microscopic patterns at pH 8.3 were not shown to save space. The orientation of PLLHBr molecules at the air–liquid interface is known to be enhanced at alkaline solutions by the depression of the dissociation of the primary amino groups of the side chains, resulting in the oriented parallel standing of the amino moieties up in the air phase [61]. Insensitivity of the dissipative patterns on pH supports, therefore, that the crystal structure is formed favorably at the air–liquid and further liquid–substrate interfaces in the whole process of dryness.

Concluding remarks

In order to know the relationship between the dissipative crystallization and the molecular stereospecificity, drying

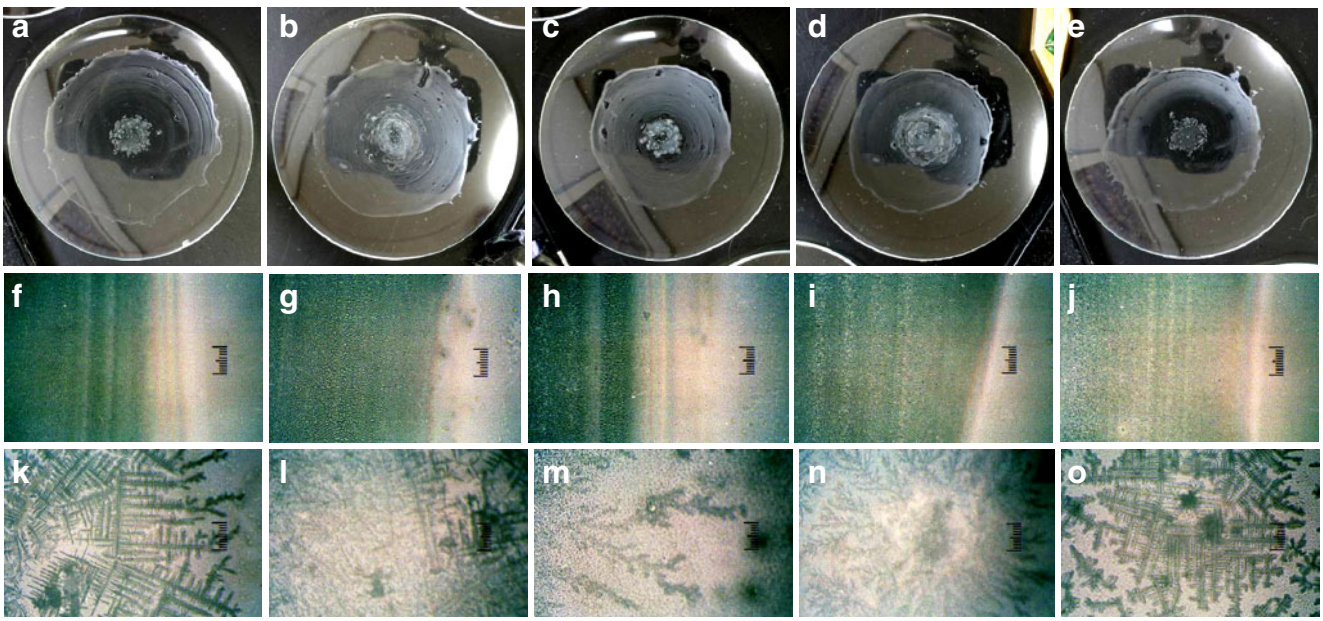

Fig. 8 Macroscopic (*a–e*) and microscopic drying patterns of aqueous PDLHBr + PLLHBr in a watch glass at 24 °C. [PDLHBr] + [PLLHBr] = 0.001 monoM, pH 6.6, 0.1 ml. *a* [PDLHBr]/[PLLHBr] = 1:0, *b* 3:1, *c* 1:1, *d* 1:3, *e* 0:1. *f* [PDLHBr]/[PLLHBr] = 1:0, *g* 3:1, *h* 1:1, *i* 1:3, *j* 0:1, edge area; full scale is 100 μm. *k* [PDLHBr]/[PLLHBr] = 1:0, *l* 3:1, *m* 1:1, *n* 1:3, *o* 0:1, central area; full scale is 100 μm

patterns of aqueous solutions of poly-D-lysine and poly-L-lysine and their low-molecular-weight analogs were studied in this work. Several important results were obtained. Firstly, morphology of the dried crystals changed as a function of the distance from the center of the dried film, which is the typical feature of the dissipative crystallization found hitherto. Secondary, morphology of D- and L-isomers were quite similar to each other for both the polymers and analogs. Size of the broad rings was also independent of the stereospecificity. Thirdly, formation of the stereo-complex between poly-D-lysine and poly-L-lysine is not plausible. The reliable evidences supporting stereospecific effects between poly-D-lysine and poly-L-lysine were not obtained in this work.

Acknowledgments Financial supports from the Ministry of Education, Culture, Sports, Science and Technology, Japan and Japan Society for the Promotion of Science are greatly acknowledged for Grants-in-Aid for Exploratory Research (17655046 to T.O.) and Scientific Research (B) (18350057 to T.O. and 19350110 to A.T.). Research fund from Rex Co. (Tokyo) to T.O. (Institute for Colloidal Organization) is also highly thanked.

References

1. Okubo T (2006) Molecular and colloidal electro-optics. In: Stoylov SP, Stoimenova MV (eds) Taylor & Francis, New York, p 573
2. Okubo T (2008) Nanoparticles: syntheses, stabilization, passivation and functionalization. In: Nagarajan R, Hatton TA (eds) ACS Book, Washington, p 256
3. Okubo T (2010) Macromol Symp 288:67
4. Gribbin G (1999) Almost everyone's guide to science. The universe, life and everything. Yale University Press, New Haven
5. Ball P (1999) The self-made tapestry. Pattern formation in nature. Oxford University Press, Oxford
6. Terada T, Yamamoto R, Watanabe T (1934) Sci Paper Inst Phys Chem Res Jpn 27:173, Proc Imper Acad Tokyo 10:10
7. Terada T, Yamamoto R, Watanabe T (1934) Sci Paper Inst Phys Chem Res Jpn 27:75
8. Nakaya U (1947) Memoirs of Torahiko Terada (Japanese). Kobunsya, Tokyo
9. Okubo T, Kimura H, Kimura T, Hayakawa F, Shibata T, Kimura K (2005) Colloid Polym Sci 283:1
10. Okubo T (2006) Colloid Polym Sci 285:225
11. Okubo T (2009) Colloid Polym Sci 287:167
12. Deegan RD, Bakajin O, Dupont TF, Huber G, Nagel SR, Witten TA (1997) Nature 389:827
13. Okubo T, Okamoto J, Tsuchida A (2009) Colloid Polym Sci 287:351
14. Okubo T (2009) Colloid Polym Sci 287:645
15. Okubo T, Okamoto J, Tsuchida A (2008) Colloid Polym Sci 286:1123
16. Okubo T (2008) Colloid Polym Sci 286:1307
17. Okubo T (2008) Colloid Polym Sci 286:1527
18. Palmer HJ (1976) J Fluid Mech 75:487
19. Anderson DM, Davis SH (1995) Phys Fluids 7:248
20. Pouth AF, Russel WB (1998) AIChEJ 44:2088
21. Burelbach JP, Bankoff SG (1998) J Fluid Mech 195:463
22. Deegan RD, Bakajin O, Dupont TF, Huber G, Nagel SR, Witten TA (2000) Phys Rev E 62:756
23. Fischer BJ (2002) Langmuir 18:60
24. Okubo T (2006) Colloid Polym Sci 284:1191
25. Okubo T (2006) Colloid Polym Sci 284:1395
26. Okubo T, Okamoto J, Tsuchida A (2007) Colloid Polym Sci 285:967
27. Okubo T (2007) Colloid Polym Sci 285:1495
28. Okubo T, Okamoto J, Tsuchida A (2008) Colloid Polym Sci 286:385
29. Okubo T, Okamoto J, Tsuchida A (2008) Colloid Polym Sci 286:941
30. Yamaguchi T, Kimura K, Tsuchida A, Okubo T, Matsumoto M (2005) Colloid Polym Sci 283:1123
31. Okubo T (2006) Colloid Polym Sci 285:331
32. Vanderhoff JW (1973) J Polym Sci Symp 41:155
33. Nicolis G, Prigogine I (1977) Self-organization in non-equilibrium systems. Wiley, New York
34. Ohara PC, Heath JR, Gelbart WM (1997) Angew Chem 109:1120
35. Maenosono S, Dushkin CD, Saita S, Yamaguchi Y (1999) Langmuir 15:957
36. Nikoobakht B, Wang ZL, El-Sayed MA (2000) J Phys Chem 104:8635
37. Ung T, Litz-Marzan LM, Mulvaney P (2001) J Phys Chem B 105:3441
38. Okubo T, Okuda S, Kimura H (2002) Colloid Polym Sci 280:454
39. Okubo T, Kimura K, Kimura H (2002) Colloid Polym Sci 280:1001
40. Okubo T, Kanayama S, Kimura K (2004) Colloid Polym Sci 282:486
41. Okubo T, Yamada T, Kimura K, Tsuchida A (2005) Colloid Polym Sci 283:1007
42. Okubo T, Nozawa M, Tsuchida A (2007) Colloid Polym Sci 285:827
43. Okubo T, Kimura K, Tsuchida A (2007) Colloids Surf B Biointerf 56:201
44. Okubo T, Nakagawa N, Tsuchida A (2007) Colloid Polym Sci 285:1247
45. Okubo T, Kimura K, Tsuchida A (2008) Colloid Polym Sci 286:621
46. Okubo T, Otake A, Tsuchida A (2009) Colloid Polym Sci 287:1435
47. Okubo T, Kanayama S, Ogawa H, Hibino M, Kimura K (2004) Colloid Polym Sci 282:230
48. Okubo T, Onoshima D, Tsuchida A (2007) Colloid Polym Sci 285:999
49. Okubo T, Ogawa H, Tsuchida A (2010) Colloid Polym Sci 288:245
50. Shimomura M, Sawadaishi T (2001) Curr Opin Coll Interf Sci 6:11
51. Okubo T, Yamada T, Kimura K, Tsuchida A (2006) Colloid Polym Sci 284:396
52. Kimura K, Kanayama S, Tsuchida A, Okubo T (2005) Colloid Polym Sci 283:898
53. Okubo T, Shinoda C, Kimura K, Tsuchida A (2005) Langmuir 21:9889
54. Okubo T, Itoh Emi, Tsuchida A, Kokufuta E (2006) Colloid Polym Sci 285:339
55. Okubo T, Okamoto J, Tsuchida A (2010) Colloid Polym Sci 288:189
56. Okubo T, Yokota N, Tsuchida A (2007) Colloid Polym Sci 285:1257
57. Okubo T, Okamoto J, Takahashi S, Tsuchida A (2009) Colloid Polym Sci 287:933
58. Okubo T, Hagiwara A, Kitano H, Okamoto J, Takahashi S, Tsuchida A (2009) Colloid Polym Sci 287:1155
59. Ikada Y, Jamshidi K, Tsuji H, Hyon SH (1987) Macromolecules 20:904
60. Tsuji H, Horii F, Hyon SH, Ikada Y (1991) Macromolecules 24:2719
61. Okubo T, Kobayashi K (1998) J Colloid Interf Sci 205:433